

Preliminary Simulation on Jet Breakup Experiment Using High Accuracy Kernel Correction Scheme for Smoothed Particle Hydrodynamics

Hae Yoon Choi^a, Eung Soo Kim^{a*}

^a Department of Nuclear Engineering, Seoul National University, 1 Gwanak-ro, Gwanak-gu, Seoul, South Korea
*Corresponding author: kes7741@snu.ac.kr

1. Introduction

At severe accident in light water reactor, the molten core materials (corium) can be erupted into water pool which exists in-vessel and ex-vessel. In this process, the fuel-coolant interaction (FCI) occurs and much debris can be formed and fragmented. (Fig. 1) Enormous steam could be generated in the pool due to the hot core melts, which may lead to steam explosion. Since these series of processes are influenced by the fragmented debris and the vapor produced in the pool, the evaluation of the two factors is important for the nuclear safety perspective. [1]

When simulating the multi-fluid components like FCI phenomenon using Smoothed Particle Hydrodynamics (SPH) code, numerical errors occur in the kernel approximation at the interface or free surface of flows. Several correction methods to resolve the approximation error have been proposed in the past years, but there are disadvantages of high cost calculation when calculating a multi-dimensional inverse matrix, and an instability problem when matrix is ill-posed.

Therefore, this study presented a method which can easily correct a kernel derivative for computational efficiency and cost, and FCI phenomenon simulation was carried out using the particle-based simulation code, SOPHIA, to which the new correction method was applied. And the simulation results were compared with those of experiment.

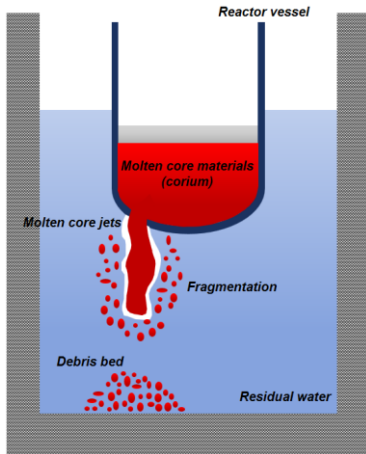


Fig 1. A schematic of FCI phenomenon

2. SPH Numerical Method

2.1 SPH basics

The SPH method is one of the Lagrangian analysis methods, which analyzes the fluid flows by calculating

the motion of individual particles. The particles have each property and are calculated through the weight function over the neighboring particles. The weight function is defined as a kernel function which has a smoothing length. This SPH method has advantages in handling free surface flow, multi-fluid (phase) flow, and high deformable geometry due to its Lagrangian nature.

The SPH approximation is performed by discretizing the kernel function which has the characteristics of the delta function.

$$f(r_i) = \sum_j \frac{m_j}{\rho_j} f_j W(r_i - r_j) \quad (1)$$

f_i is a function at the position i , $W(r_i - r_j)$ is a kernel function, j is a neighboring particle within the smoothing length, and m, ρ means mass and density, respectively.

The first derivative of the field function $f(r)$ is expressed as a function of kernel derivatives for all the particles in the support domain of particle i . [2]

$$\nabla f(r_i) = \sum_j \frac{m_j}{\rho_j} f_j \nabla W(r_i - r_j) \quad (2)$$

2.2 Governing equations

The SPH method basically satisfies the conservation of mass and momentum, and can be expressed in the form of equations (3) and (4). There are two approaches for density calculation, the first is mass summation and the second is continuity equation. In this study, mass summation is used.

$$\frac{d\rho}{dt} = -\rho \nabla \cdot \vec{u} \quad (3)$$

$$\frac{d\vec{u}}{dt} = -\frac{1}{\rho} \nabla P + \frac{\mu}{\rho} \nabla^2 \vec{u} + \vec{g} \quad (4)$$

\vec{u}, P, μ, \vec{g} denote velocity field, pressure, dynamic viscosity, and gravitational constant, respectively.

Table 1. shows the SPH expression of the governing equations. In the general SPH method, the calculation is carried out assuming weak compressibility of the fluid, so Tait equation is used for equation of state (EOS).

2.3 Multi-fluid models

In multi-fluid calculation, a discontinuity of physical properties occurs at the fluid interface. Since the SPH pressure force calculation is a function of density, large density difference near the boundary cause non-physical pressure force.

Table 1. SPH Formulations

Mass Conservation	
Mass summation	$\rho_i = \sum_j m_j W_{ij}$
Continuity equation	$\left(\frac{d\rho}{dt}\right)_i = \rho_i \sum_j \frac{m_j}{\rho_j} (\bar{u}_i - \bar{u}_j) \cdot \nabla W_{ij}$
Momentum Conservation	
Pressure force	$\left(\frac{d\bar{u}}{dt}\right)_i = \sum_j -\frac{m_j}{\rho_i \rho_j} (P_j + P_i) \nabla W_{ij}$
Viscous force	$\left(\frac{d\bar{u}}{dt}\right)_i = \sum_j -\frac{4m_j}{\rho_i \rho_j} \frac{\mu_i \mu_j}{\mu_i + \mu_j} \frac{\bar{r}_{ij} \cdot \nabla W_{ij}}{r_{ij}^2 + \varepsilon^2} (\bar{u}_i - \bar{u}_j)$
Equation of State	
	$P = \frac{c_0^2 \rho_0}{\gamma} \left[\left(\frac{\rho}{\rho_0}\right)^\gamma - 1 \right]$

Therefore, a normalized-density formulation is introduced to ensure stability by replacing the density (ρ) with the normalized density (ρ/ρ_0).

$$\left(\frac{\rho}{\rho_0}\right)_i = \sum_j \frac{m_j}{\rho_{0,j}} W_{ij} \quad (5)$$

$$\frac{d}{dt} \left(\frac{\rho}{\rho_0}\right)_i = -\left(\frac{\rho_i}{\rho_{0,i}}\right) \sum_j \frac{m_j}{\rho_j} (\bar{u}_i - \bar{u}_j) \cdot \nabla W_{ij} \quad (6)$$

Since not only density, but also viscosity and heat transfer coefficient are discontinuous at the interface, the thermal conductivity in the conduction equation is also applied by transforming the shape as in the previous viscous force calculation formulation.

$$\left(\frac{dh}{dt}\right)_i = \sum_j \frac{4m_j}{\rho_i \rho_j} \frac{k_i k_j}{k_i + k_j} \frac{\bar{r}_{ij} \cdot \nabla W_{ij}}{r_{ij}^2 + \varepsilon^2} (T_i - T_j) \quad (7)$$

3. Simplified Kernel Gradient Correction

For the accurate SPH approximation, the spatial integral of the kernel function should be 1.

$$\int_{\Omega} W(r - r', h) d\Omega = 1 \quad (8)$$

$$\sum_j \frac{m_j}{\rho_j} W(r_i - r_j) = 1 \quad (9)$$

The above equations are referred as unity condition, and generally satisfied inside region of the fluid for ideal conditions. However, this condition is not satisfied near the boundary where the particle distribution is non-

uniform or the analysis area is cut off. (Fig. 2) This causes not only the degradation of calculation accuracy, but also numerical instability. [3] And, the errors also occur in the SPH approximation of the kernel derivative. In order to resolve these errors, several studies have been carried out in the past, and various kernel gradient correction (KGC) methods have been proposed. A brief description of KGC method is given in the next section.

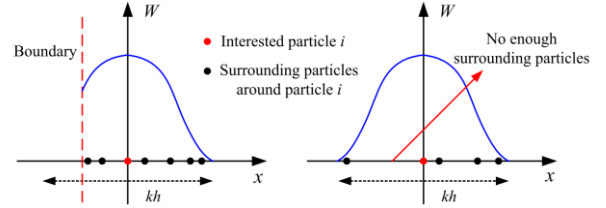


Fig 2. Truncated and non-uniform particle distribution

3.1 Conventional kernel gradient correction

Chen (2000) proposed a corrected SPH (CSPM) from Taylor series. CSPM provides better results than conventional SPH method by solving particle deficiency problems near the boundary. [4] In the similar way, Liu et al (2006) proposed a finite particle method (FPM), which is known to have greater accuracy due to its simultaneous calculations on the value of the function itself and the gradient term. [5] Because the principal component direction plays a major role in the correction, decoupled FPM (DFPM) which considers only the principal component of FPM matrix was proposed by Zhang (2018). [6] On the other hand, Huang (2016) proposed a Kernel Gradient Free (KGF) method by excluding the kernel gradient itself that causes errors. [7] Table 2. shows the expression of several kernel gradient correction methods.

The above methods improves the results in the vicinity of the interface by correcting the particle inconsistency, however, it is necessary to perform multi-dimensional inverse matrix calculation, and in the case of ill-posed, there is a problem that the inverse matrix does not exist, so the calculation cost can be high and somewhat inefficient.

3.2 Simplified kernel gradient correction

Therefore, a simplified correction method was introduced to perform the calculation more efficiently. Using the central difference approximation from Taylor series, the eqn. (10) can be derived.

$$\begin{aligned} \left(\frac{\partial f}{\partial x}\right)_i &\approx \frac{f(i_R) - f(i_L)}{2\Delta x} \\ &= \frac{1}{2\Delta x} \left[\sum_j \frac{m_j}{\rho_j} f_j W_{i+\Delta x} - \sum_j \frac{m_j}{\rho_j} f_j W_{i-\Delta x} \right] \end{aligned} \quad (10)$$

i_R, i_L indicate the position where i particle moved very slightly in the positive/negative direction.

Table 2. The several kernel gradient correction methods

Correction method	Matrix expression
CSPM	$\begin{bmatrix} f_{x,i} \\ f_{y,i} \\ f_{z,i} \end{bmatrix} = \begin{bmatrix} \sum_j (x_j - x_i) W_x \frac{m_j}{\rho_j} & \sum_j (y_j - y_i) W_x \frac{m_j}{\rho_j} & \sum_j (z_j - z_i) W_x \frac{m_j}{\rho_j} \\ \sum_j (x_j - x_i) W_y \frac{m_j}{\rho_j} & \sum_j (y_j - y_i) W_y \frac{m_j}{\rho_j} & \sum_j (z_j - z_i) W_y \frac{m_j}{\rho_j} \\ \sum_j (x_j - x_i) W_z \frac{m_j}{\rho_j} & \sum_j (y_j - y_i) W_z \frac{m_j}{\rho_j} & \sum_j (z_j - z_i) W_z \frac{m_j}{\rho_j} \end{bmatrix}^{-1} \begin{bmatrix} \sum_j [f_j - f_i] W_x \frac{m_j}{\rho_j} \\ \sum_j [f_j - f_i] W_y \frac{m_j}{\rho_j} \\ \sum_j [f_j - f_i] W_z \frac{m_j}{\rho_j} \end{bmatrix}$
FPM	$\begin{bmatrix} f_i \\ f_{x,i} \\ f_{y,i} \\ f_{z,i} \end{bmatrix} = \begin{bmatrix} \sum_j W \frac{m_j}{\rho_j} & \sum_j (x_j - x_i) W \frac{m_j}{\rho_j} & \sum_j (y_j - y_i) W \frac{m_j}{\rho_j} & \sum_j (z_j - z_i) W \frac{m_j}{\rho_j} \\ \sum_j W_x \frac{m_j}{\rho_j} & \sum_j (x_j - x_i) W_x \frac{m_j}{\rho_j} & \sum_j (y_j - y_i) W_x \frac{m_j}{\rho_j} & \sum_j (z_j - z_i) W_x \frac{m_j}{\rho_j} \\ \sum_j W_y \frac{m_j}{\rho_j} & \sum_j (x_j - x_i) W_y \frac{m_j}{\rho_j} & \sum_j (y_j - y_i) W_y \frac{m_j}{\rho_j} & \sum_j (z_j - z_i) W_y \frac{m_j}{\rho_j} \\ \sum_j W_z \frac{m_j}{\rho_j} & \sum_j (x_j - x_i) W_z \frac{m_j}{\rho_j} & \sum_j (y_j - y_i) W_z \frac{m_j}{\rho_j} & \sum_j (z_j - z_i) W_z \frac{m_j}{\rho_j} \end{bmatrix}^{-1} \begin{bmatrix} \sum_j f_j W \frac{m_j}{\rho_j} \\ \sum_j f_j W_x \frac{m_j}{\rho_j} \\ \sum_j f_j W_y \frac{m_j}{\rho_j} \\ \sum_j f_j W_z \frac{m_j}{\rho_j} \end{bmatrix}$
DFPM	$\begin{bmatrix} f_i \\ f_{x,i} \\ f_{y,i} \\ f_{z,i} \end{bmatrix} = \begin{bmatrix} \sum_j W \frac{m_j}{\rho_j} & 0 & 0 & 0 \\ 0 & \sum_j (x_j - x_i) W_x \frac{m_j}{\rho_j} & 0 & 0 \\ 0 & 0 & \sum_j (y_j - y_i) W_y \frac{m_j}{\rho_j} & 0 \\ 0 & 0 & 0 & \sum_j (z_j - z_i) W_z \frac{m_j}{\rho_j} \end{bmatrix}^{-1} \begin{bmatrix} \sum_j f_j W \frac{m_j}{\rho_j} \\ \sum_j f_j W_x \frac{m_j}{\rho_j} \\ \sum_j f_j W_y \frac{m_j}{\rho_j} \\ \sum_j f_j W_z \frac{m_j}{\rho_j} \end{bmatrix} = \begin{bmatrix} (\sum_j f_j W \frac{m_j}{\rho_j}) / (\sum_j W \frac{m_j}{\rho_j}) \\ (\sum_j [f_j - f_i] W_x \frac{m_j}{\rho_j}) / (\sum_j (x_j - x_i) W_x \frac{m_j}{\rho_j}) \\ (\sum_j [f_j - f_i] W_y \frac{m_j}{\rho_j}) / (\sum_j (y_j - y_i) W_y \frac{m_j}{\rho_j}) \\ (\sum_j [f_j - f_i] W_z \frac{m_j}{\rho_j}) / (\sum_j (z_j - z_i) W_z \frac{m_j}{\rho_j}) \end{bmatrix}$
KGF	$\begin{bmatrix} f_i \\ f_{x,i} \\ f_{y,i} \\ f_{z,i} \end{bmatrix} = \begin{bmatrix} \sum_j W \frac{m_j}{\rho_j} & \sum_j (x_j - x_i) W \frac{m_j}{\rho_j} & \sum_j (y_j - y_i) W \frac{m_j}{\rho_j} & \sum_j (z_j - z_i) W \frac{m_j}{\rho_j} \\ \sum_j (x_j - x_i) W \frac{m_j}{\rho_j} & \sum_j (x_j - x_i)(x_j - x_i) W \frac{m_j}{\rho_j} & \sum_j (y_j - y_i)(x_j - x_i) W \frac{m_j}{\rho_j} & \sum_j (z_j - z_i)(x_j - x_i) W \frac{m_j}{\rho_j} \\ \sum_j (y_j - y_i) W \frac{m_j}{\rho_j} & \sum_j (x_j - x_i)(y_j - y_i) W \frac{m_j}{\rho_j} & \sum_j (y_j - y_i)(y_j - y_i) W \frac{m_j}{\rho_j} & \sum_j (z_j - z_i)(y_j - y_i) W \frac{m_j}{\rho_j} \\ \sum_j (z_j - z_i) W \frac{m_j}{\rho_j} & \sum_j (x_j - x_i)(z_j - z_i) W \frac{m_j}{\rho_j} & \sum_j (y_j - y_i)(z_j - z_i) W \frac{m_j}{\rho_j} & \sum_j (z_j - z_i)(z_j - z_i) W \frac{m_j}{\rho_j} \end{bmatrix}^{-1} \begin{bmatrix} \sum_j f_j W \frac{m_j}{\rho_j} \\ \sum_j f_j (x_j - x_i) W \frac{m_j}{\rho_j} \\ \sum_j f_j (y_j - y_i) W \frac{m_j}{\rho_j} \\ \sum_j f_j (z_j - z_i) W \frac{m_j}{\rho_j} \end{bmatrix}$

In the SPH approximation, the correction can be performed by dividing the kernel function with the unity condition of eqn. (9). (Shepard filter) With this method, eqn. (11) can be expressed by dividing eqn. (10) with the Shepard filter.

$$\left(\frac{\partial f}{\partial x}\right)_i = \frac{1}{2\Delta x} \left[\frac{\sum_j \frac{m_j}{\rho_j} f_j W_{i+\Delta x}}{\sum_j \frac{m_j}{\rho_j} W_{i+\Delta x}} - \frac{\sum_j \frac{m_j}{\rho_j} f_j W_{i-\Delta x}}{\sum_j \frac{m_j}{\rho_j} W_{i-\Delta x}} \right] \quad (11)$$

Because Δx is very small, $O(\Delta x^2)$ can be neglected. Then, for the final form of the simplified correction method is derived as eqn. (12).

$$\nabla f(r_i)_{new} = \frac{\sum_j \frac{m_j}{\rho_j} \nabla W_{ij}}{\sum_j \frac{m_j}{\rho_j} W_{ij}} \left[\frac{\sum_j \frac{m_j}{\rho_j} f_j \nabla W_{ij}}{\sum_j \frac{m_j}{\rho_j} W_{ij}} - \frac{\sum_j \frac{m_j}{\rho_j} f_j W_{ij}}{\sum_j \frac{m_j}{\rho_j} W_{ij}} \right] \quad (12)$$

3.3 Evaluation

In order to evaluate the new derived correction method, comparisons were carried out for SPH summation of original form, KGF, and simplified KGC. (Eqn. 12-14)

Original form

$$\nabla f(r_i) = \sum_j \frac{m_j}{\rho_j} f_j \nabla W_{ij} \quad (13)$$

KGF form

$$\nabla f(r_i) = \sum_j \frac{m_j}{\rho_j} f_j \tilde{L} \nabla W_{ij} \quad (14)$$

Using a quadratic polynomial function the derivative of function was calculated. As shown in fig. 3, the calculated value with the correction shows much better results near the free surface than the original form. In the simplified KGC method, the degree of the correction is

slightly less than that of KGF, but the simplified KGC method has a great advantage in terms of computational efficiency and stability.

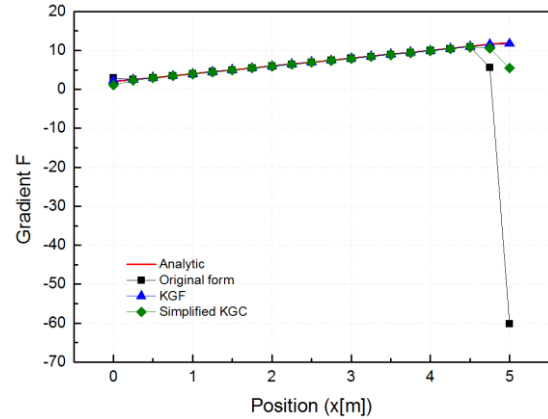


Fig 3. Comparison of the gradient calculation according to correction method

4. Jet Breakup Simulation

4.1 Reference experiment

In this study, the FCI jet breakup of two different fluids was simulated using the SOPHIA code. The experiment of Manickam et al. (2017) was selected as a reference experiment, and analysis of jet breakup process according to different jet speeds and flooded conditions was carried out. [8]

4.2 Simulation model

Fig. 4 shows the schematic of MISTEE-Jet facility simulating jet breakup at KTH. The wall is made of

plexi-glass for observation, each side of wall is 75mm and a water pool depth is 465mm, and the nozzle diameter is 5mm.

Wood's metal was used as a corium simulant, and the experimental conditions were arranged through scaling analysis of density ratio, Weber number, and Froude number. Initial temperature conditions of 16°C water pool and 91°C liquid wood's metal were given.

Using SPH code, 3D jet breakup simulations were performed according to the jet speeds (1m/s – 3m/s) and nozzle diameter conditions (5-10mm). And the total number of calculating particles is about 9 millions.

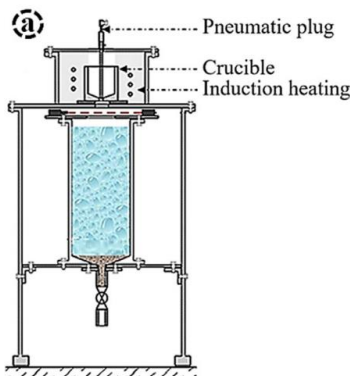


Fig 4. Schematic of MISTEE-Jet facility [8]

4.3 Result and discussion

As shown in fig. 5, the jet breakup simulation results with 1.7m/s jet speed condition are compared with the experimental data. The fragmentation of jet flow was well simulated and have good agreement with experiment.

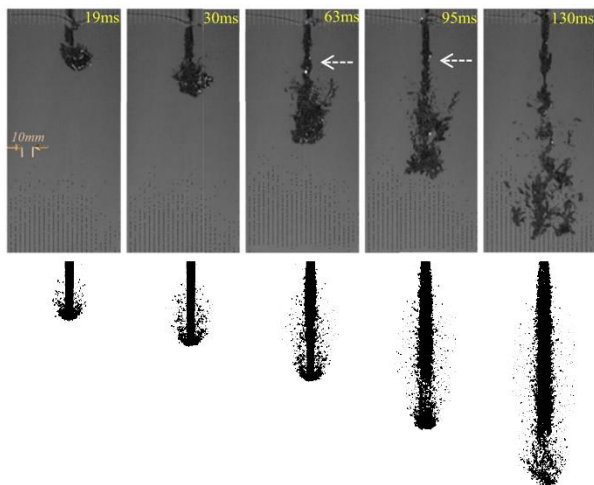


Fig 5. Comparison jet breakup simulation results with experiment (1.7m/s, fully-flooded condition)

5. Summary

In this study, a new kernel gradient correction method was proposed to resolve the numerical errors in the SPH approximation. By applying the correction, it was confirmed that the calculated derivative value near the fluid boundary was improved. In addition, jet breakup simulations using high resolution SPH code were carried out with the new correction, and results were in good agreement with those of reference experiment.

ACKNOWLEDGEMENT

This work was supported by the Nuclear Safety Research Program through the Korea Foundation Of Nuclear Safety (KoFONS) using the financial resource granted by the Nuclear Safety and Security Commission (NSSC) of the Republic of Korea. (No. 1903003)

REFERENCES

- [1] OECD/NEA SERENA Final Report, 2007. SERENA-Steam Explosion Resolution for Nuclear Applications. NEA/CSNI/R (2007)11.
- [2] G. R. Liu, M. B. Liu, "Smoothed Particle Hydrodynamics: a meshfree particle methods", 2003.
- [3] Bonet, Javier, and T-SL Lok. "Variational and momentum preservation aspects of smooth particle hydrodynamic formulations." *Computer Methods in applied mechanics and engineering* 180.1-2 (1999): 97-115.
- [4] Chen, J. K., and J. E. Beraun. "A generalized smoothed particle hydrodynamics method for nonlinear dynamic problems." *Computer Methods in Applied Mechanics and Engineering* 190.1-2 (2000): 225-239.
- [5] Liu, M. B., and Gui-Rong Liu. "Restoring particle consistency in smoothed particle hydrodynamics." *Applied numerical mathematics* 56.1 (2006): 19-36.
- [6] Zhang, Z. L., and M. B. Liu. "A decoupled finite particle method for modeling incompressible flows with free surfaces." *Applied Mathematical Modelling* 60 (2018): 606-633.
- [7] Huang, C., et al. "An improved KGF-SPH with a novel discrete scheme of Laplacian operator for viscous incompressible fluid flows." *International Journal for Numerical Methods in Fluids* 81.6 (2016): 377-396.
- [8] Manickam, Louis, Sevostian Bechta, and Weimin Ma. "On the fragmentation characteristics of melt jets quenched in water." *International Journal of Multiphase Flow* 91 (2017): 262-275.